Bull. Mater. Sci., Vol. 36, No. 3, June 2013, pp. 367–372. © Indian Academy of Sciences.

# Facile synthesis of Au/ZnO nanoparticles and their enhanced photocatalytic activity for hydroxylation of benzene

**HANG YU[1], HAI MING[1], JINGJING GONG[1], HAITAO LI[1], HUI HUANG[1], KEMING PAN[1], YANG LIU[1,*], ZHENHUI KANG[1], JIE WEI[2] and DONGTIAN WANG[2]**

[1]Institute of Functional Nano and Soft Materials (FUNSOM) and Jiangsu Key Laboratory for Carbon-based Functional Materials and Devices, Soochow University, Suzhou 215123, China

[2]Department of Chemical and Biological Engineering, Suzhou University of Science and Technology, Suzhou 215011, China

MS received 15 September 2011; revised 21 August 2012

**Abstract.** **Au/ZnO nanocomposites have been prepared by a simple chemical method. For the first time, the nanocomposites were directly used as photocatalysts for hydroxylation of aromatic hydrocarbons under UV and visible light irradiation. The results show that the as-prepared photocatalysts display high photocatalytic activity for UV and visible catalytic hydroxylation of benzene. Without the assistance of any solvent or additive, high selectivity and high conversion efficiency were still obtained. Different photocatalytic mechanisms were proposed depending on whether excitation happens on ZnO semiconductor or on the surface plasmon band of Au. The former is Au nanoparticles act as electron buffer due to irradiation by UV light and ZnO nanoparticles as reactive sites for hydroxylation of benzene, the latter is that Au nanoparticles act as light harvesters and inject electrons into ZnO conduction band and as photocatalytic sites under visible light irradiation.**

**Keywords.** **Zinc oxide; gold nanoparticles; nanocomposites; photocatalysis; visible light.**

## 1. Introduction

ZnO nanoparticles (ZnO NPs) have attracted significant attention for a long time as a kind of promising photocatalysts (Kurtz *et al* 2005) because of their nontoxic nature, low cost and unique surface chemistry properties (Kabra *et al* 2004; Akyol *et al* 2004; Chakrabarti and Dutta 2004). However, there is still much room for efficiency improvement in most photocatalytic processes using UV light and particularly visible light with ZnO photocatalyts due to their wide bandgap (3·37 eV) and high rate of electron–hole recombination. In recent years, hence the design of nanophotocatalyst (new-generation catalyst) with strong and tuneable chemical activity, specificity and selectivity has been widely attended (Bell 2003; Hughes *et al* 2005; Corma and Serna 2006; Sun and Bao 2008; Turner *et al* 2008; Kang *et al* 2009). Doping with metals (Akyol *et al* 2004; Kabra *et al* 2004; Wang 2008), particularly noble (Chakrabarti and Dutta 2004; Tarek and Anja-Verena 2009; Beqa *et al* 2011; Donkova *et al* 2011), nonmetallic elements (Kurtz *et al* 2005; Wang *et al* 2009), such as C and N, and organic dye sensitization (Hughes *et al* 2005) has been widely used to enhance visible light absorption of ZnO nanomaterials. In this regard, one interesting alternative in improving the photoactivity of ZnO NPs is the use of Au nanoparticles (Au NPs) loaded on the ZnO surface. Au is one of the important noble metal and does not undergo corrosion in photocatalytic processes. Au NPs not only provide a convenient way to direct flow of photoinduced charge carriers because of irradiation by UV light, which helps to hinder electron–hole pairs recombination, but also display a characteristic plasmon band in the visible region due to the collective excitation of electrons in Au NPs (Liu *et al* 2006; Zhang *et al* 2006). One interesting application of Au/ZnO nanocomposites is its use as is heterogeneous catalyst. In spite of the numerous work of investigating the photocatalytic and thermal catalytic activity of modified and unmodified ZnO NPs, the work investigating the photocatalytic hydroxylation of aromatic hydrocarbons upon UV and visible light irradiation with Au/ZnO nanocomposites is still very scarce.

It is well known that phenol is produced on a large scale (about 7 billion kg/year) as a chemical intermediate to many materials and useful compounds, such as plastic, nylon, herbicides and pharmaceuticals (Manfred *et al* 2004). Nowadays, most of the worldwide production of phenol is based on Cumene processes (Cumenephenol and Hock processes). However, the typical industrial technology of producing phenol not only contains complex processes, but also suffers from high temperature, large energy consumption and high cost (Fortuin and Waterman 1953). Therefore, developing one-step synthesis of phenol has attracted wide attention in the world. Several kinds of catalysts, such as titanium silicates (TS-1) and carbon nanotubes have been studied for the hydroxylation of aromatic hydrocarbons

*Author for correspondence (yangl@suda.edu.cn)

with $H_2O_2$ as oxidant directly (Bhaumik and Kumar 1995; Bhaumik *et al* 1998; Kang *et al* 2006).

In the present work, uniform ZnO NPs (a side-edge length of ∼20 nm) have been synthesized by alcoholysis and Au NPs are also loaded on the as-prepared ZnO NPs successfully. The photocatalysis of the as-prepared Au/ZnO NPs for the hydroxylation of benzene using $H_2O_2$ as oxidant have been studied upon UV and visible light irradiation without any solvent or additives. The high activity and selectivity were observed in the low-temperature interface reaction under UV and visible light irradiation. Two different operating mechanisms for photocatalytic hydroxylation of benzene are proposed depending on the excitation wavelength (UV or visible light). Noteworthily, this is the first report regarding Au/ZnO composite for photocatalytic hydroxylation of benzene with UV and visible light.

## 2. Experimental

### 2.1 *Materials*

Zinc acetate dihydrate ($Zn(Ac)_2{\cdot}2H_2O$), alcohol, the aqueous solution of hydrogen peroxide ($H_2O_2$, 30 wt%), $HAuCl_4$, sodium citrate, ascorbic acid and benzene are all of analytical grade and were purchased from Sinopharm Chemical Reagent (Shanghai, China). All of these chemicals were used without further purification.

### 2.2 *Synthesis of ZnO NPs and Au/ZnO nanocomposites*

In a typical process, 30 mL $Zn(Ac)_2{\cdot}2H_2O$ (0·25 M) ethanol solution placed in a teflon-lined stainless steel autoclave (50 mL) was heated and kept at a constant temperature of 160 °C for 6 h. After hydrothermal treatment, ZnO products were collected by sedimentation and washed several times with deionized water and absolute ethanol. Then the collected sample was vacuum-dried at 60 °C for 24 h.

ZnO NPs (0·3 g) was immersed into a mixture of 1·0 mL sodium citrate (0·01 M), 1·0 mL $HAuCl_4$ (0·01 M), 2·0 mL ascorbic acid (0·01 M) and 20 mL deionized water under magnetic stirring at room temperature for 3 h. The obtained powder was separated by centrifugation and washed with deionized water and absolute ethanol and then dried in vacuum oven at 60 °C for 24 h.

### 2.3 *Photocatalytic activity*

Typically, the reagent of benzene was added to a mixture of aqueous solution of $H_2O_2$ (10 mL, 30 wt%) and 0·1 g photocatalysts (as-prepared ZnO NPs or Au/ZnO nanocomposites). The mixture was refluxed in a round-bottomed flask and mixed thoroughly under vigorous magnetic stirring. The flask was irradiated by UV or visible light in a black room. The desired volume of mixture was gathered from the reactor at 2, 4, 6, 8, 10 and 24 h, respectively. All of the oxidation products were monitored with a gas chromatography (Agilent 7890A) equipped with a flame ionization detector (FID).

### 2.4 *Characterization*

X-ray powder diffraction (XRD) patterns were recorded by using a X'Pert-ProMPD (Holand) D/max-$\gamma$AX-ray diffractometer with $CuK_\alpha$ radiation ($\lambda = 0{\cdot}154178$ nm). Scanning electron microscopy (SEM) images and energy dispersive X-ray (EDX) spectroscopy were collected under a FEI-quanta200 scanning electron microscope with acceleration voltage of 20 kV. Transmission electron microscopy (TEM) and high resolution transmission electron microscopy (HRTEM) images were obtained with FEI/Philips Tecnai 12 BioTWIN transmission electron microscope operating on 200 kV and specimens were dispersed in ethanol and then a drop of solution was placed on a holey carbon film electron microscope grid and the solvent was allowed to evaporate. Room temperature UV–Vis absorption was recorded on a Lambda 750 (PerkinElmer) spectrophotometer in the wavelength range of 200–800 nm. Gas chromatography was performed in Varian 3400 GC column with a cross-linked 5% PhMe silicone column (25 m × 0·20 mm × 0·33 μm) and FID detector under the following conditions: carrier gas ($N_2$) at 140 K; temperature program 60 °C, 1 min, 15 °C/min, 180 °C, 15 min; split ratio, 10:1; injector, 300 °C and detector, 300 °C.

## 3. Results and discussion

### 3.1 *X-ray powder diffraction*

XRD was used to check the purity and crystallinity of ZnO nanocrystals and detect the presence of Au NPs. In figure 1(a), XRD pattern of as-prepared ZnO nanocrystals corresponds to a typical diffraction pattern of wurtzite ZnO phase as cross-referenced to JCPDS 36-1451 card, while no other peaks for impurities are observed. Figure 1(b) depicts XRD pattern of Au/ZnO composite. It was found that (111), (200) and (220) diffraction peaks, which are attributed to the typical cubic-phase Au (JCPDS no. 04-0784), can be readily observed in figure 1(b) (Strunk *et al* 2009; Li *et al* 2011). It indicates that the composite is composed of wurtzite hexagonal-structured ZnO and cubic-phase Au.

### 3.2 *Scanning and transmission electron microscopies*

Figure 2(a) depicts representative SEM image of the as-prepared Au/ZnO sample. This image indicates that the highly dispersed nanoparticles have been obtained with an average diameter of ∼20 nm. EDX spectrum (corresponding to figure 2a) is used to analyse the elemental composition of the hybrid particles (figure 2b). The peaks of Zn, O, Au and Si can be clearly seen in EDX spectrum and Si from the substrate specimen, which indicates that the sample is formed of Au and ZnO phases. Further inductive

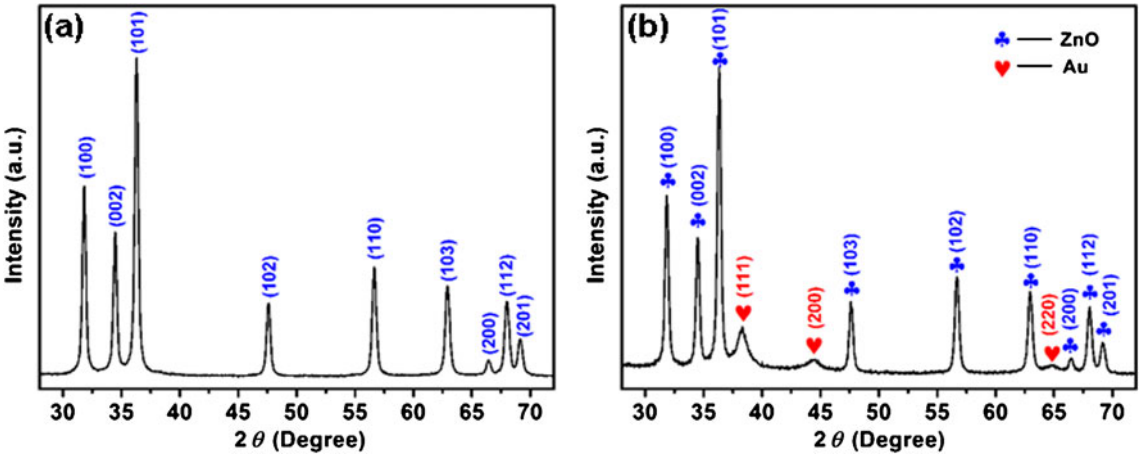


**Figure 1.** XRD patterns of (**a**) ZnO nanoparticles and (**b**) Au/ZnO composites.

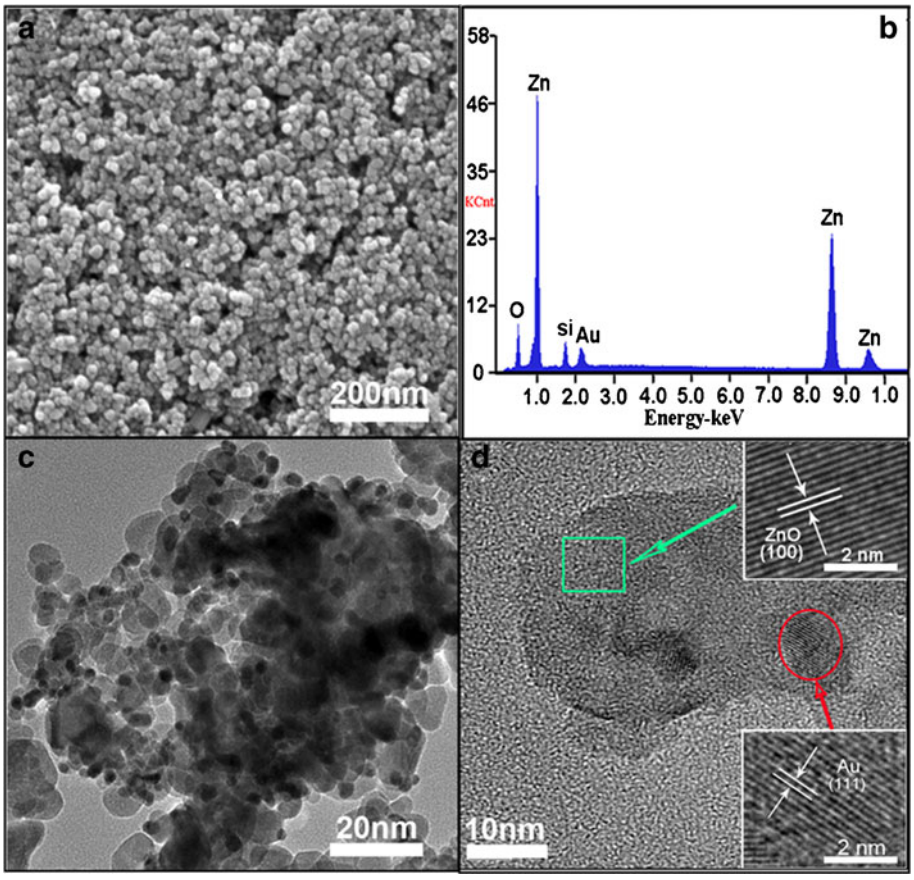


**Figure 2.** (**a**) SEM image of as-prepared Au/ZnO nanoparticles, (**b**) EDX spectrum corresponding to samples shown in (**a**) SEM image, (**c**) TEM image of as-prepared Au/ZnO composites and (**d**) magnified TEM image of Au/ZnO nanoparticles; insets show HRTEM images corresponding to line drawn.

coupled plasma (ICP) element analysis of present Au/ZnO sample indicated that Au count is about 4·8 wt%. Typical TEM image of the nanocomposites is presented in figure 2(c), in which we can see clearly that the surface of ZnO nanocrystal is decorated with many Au NPs. In order to further prove the presence of Au and ZnO in the composites, TEM images with higher magnification are shown in figure 2(d). The insets (figure 2d) are HRTEM images corresponding to lines drawn in figure 2(d) and highlight the lattice fringes in crystalline domain of the composites. The

lattice fringes from the up-inset and down-inset in figure 2(d) were calculated to be about 0·281 and 0·235 nm, respectively. The lattices correspond to (100) plane of wurtzite ZnO phase and (111) plane of cubic Au phase, respectively. From the above results, we can see that the highly dispersed ZnO/Au photocatalyst has been obtained.

### 3.3 *UV–Vis absorption*

Figure 3 presents UV–Vis spectra of the as-prepared ZnO NPs and Au/ZnO composites. Both of the samples (ZnO NPs and Au/ZnO composites) exhibit a representative absorption with intense transition in UV region of the spectra that is due to the bandgap transition of ZnO semiconductor. The direct bandgap energy of about 3·3 eV for as-prepared ZnO NPs and Au/ZnO composites can be estimated from figure 3 (convert the units, intercept of the tangents to the plots of $(\alpha h\nu)^2$ vs photon energy and then obtain the optical bandgap by extrapolating a line from the maximum slope of the curve to the $x$-axis). From curve $b$ in figure 3, a typical absorption of the gold surface plasmon band can be easily observed in the visible region between 500 and 650 nm. This not only confirms that Au NPs have been successfully supported on the surface of ZnO nanocrystals, but also confirms that Au/ZnO composites have much stronger absorption for visible light than that of ZnO NPs, which obviously implies that Au/ZnO composites possess higher photoactivity for target photocatalytic reaction than that of bare ZnO NPs under visible light irradiation (Silva *et al* 2011). In addition, from figure 3, we can see that the presence of Au NPs also make ZnO NPs to have a stronger absorption intensity in the UV region than bare ZnO nanocrystals, which suggests that Au/ZnO composites have higher photoactivity than pure ZnO NPs under UV irradiation (Xu *et al* 2010).

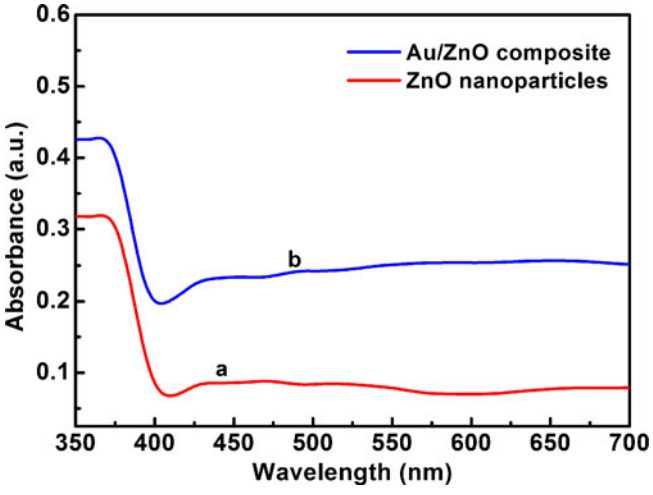


**Figure 3.** UV–Vis spectra of (**a**) ZnO nanoparticles and (**b**) Au/ZnO composites.

### 3.4 *Catalytic activity of Au/ZnO nanocomposites for hydroxylation of benzene*

The strong absorption of Au surface plasmon band of the as-prepared Au/ZnO composites was observed in figure 3, which implies that the hybrid displays significant photocatalytic activity in visible region. Hence, in the first stage, the photocatalytic activity of Au/ZnO composites was investigated for hydroxylation of benzene in the absence of solvent upon irradiation with visible light with $H_2O_2$ as oxidant, using Au/ZnO nanocomposites and ZnO NPs as catalysts, respectively. A comparison of the selectivity (▲, ▼ in figure 4a) and conversion (▲, ▼ in figure 4b) to phenol for hydroxylation of benzene upon visible light irradiation with Au/ZnO composites and ZnO NPs are shown in figure 4. As it can be seen, the selectivity to phenol always maintains at 100% in the reaction range and the percentage of conversion to phenol increases with the reaction time increasing with Au/ZnO composites and ZnO NPs, respectively after

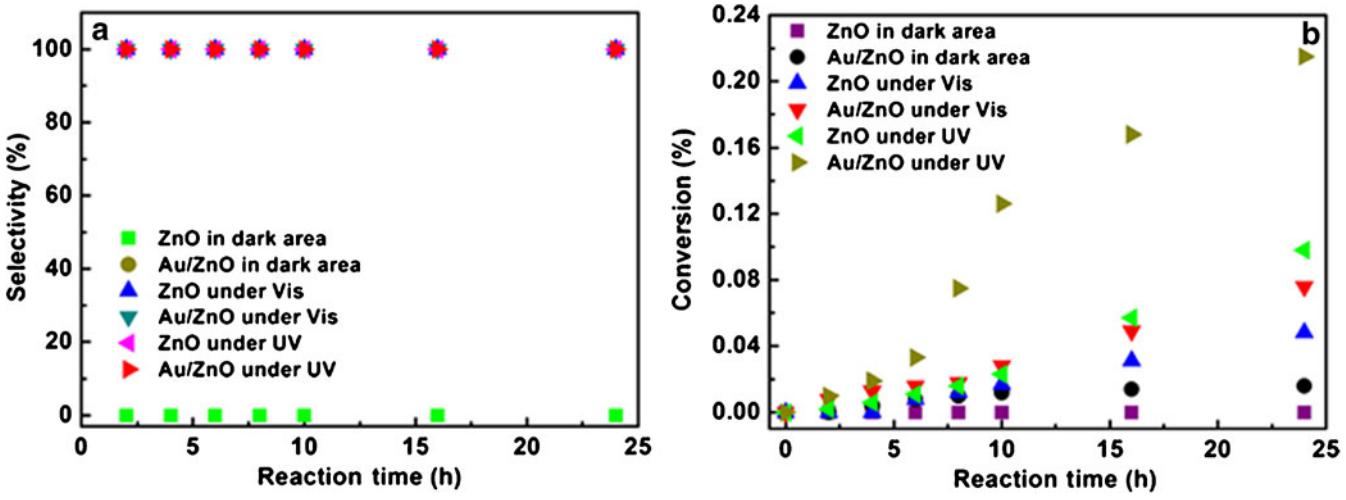


**Figure 4.** (**a**) Selectivities and (**b**) conversions to phenol for photocatalytic hydroxylation of benzene under different light source irradiations.

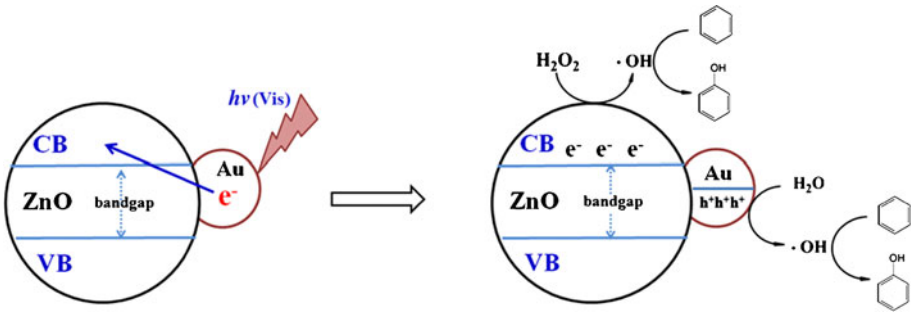


**Scheme 1.** Proposed mechanism of photocatalytsis of as-prepered Au/ZnO composites upon excitation of visible light.

24 h, the conversion can reach 7·6% with Au/ZnO composites while the conversion using ZnO NPs as catalyst is only 4·8%. It is obviously demonstrated that the Au/ZnO composites possess better photocatalytic performance for hydroxylation of benzene than that of ZnO NPs. Simultaneously, we conclude from the results of the experiments that the stabilized, separated and high Au-content of Au NPs are responsible for the high conversion efficiency, while the unique feature of ZnO nanocrystals alone are for the high selectivity to phenol.

To further elucidate the catalytic ability of Au/ZnO nanocomposites for hydroxylation of benzene under visible light irradiation, similar experiments for hydroxylation of benzene in dark area were performed using Au/ZnO composites and ZnO NPs as catalysts, respectively. Details of the selectivities (■, ● in figure 4a) and conversions (■, ● in figure 4b) for hydroxylation of benzene are shown in figure 4. As it can be seen that bare ZnO NPs are devoid of photocatalytic activity under dark area and Au/ZnO composites have lower photocatalytic ability than that in visible light irradiation. However, the selectivity to phenol for hydroxylation of benzene with Au/ZnO composites and ZnO NPs also maintains 100%. The results conformed that visible light has significant influence on conversion of the hydroxylation reaction while using the as-prepared photocatalysts.

The results of the photocatalytic reactions under visible light irradiation can be explained by the mechanism displayed in scheme 1. As it can be seen, under visible photoexcitation of Au NPs, electrons emitted from Au NPs are injected into the ZnO conduction band leading to the generation of holes in Au NPs and electrons in the semiconductor ZnO conduction band (Silva *et al* 2011). The holes in Au NPs conduction band are beneficial for generating a larger amount of photocatalytic species (such as O*) on Au surface (Xu *et al* 2010), leading to the high photocatalytic activity of Au/ZnO composites for hydroxylation of benzene as compared to ZnO NPs alone. Evidence supporting the proposed mechanism is the fact that the photocatalytic response for hydroxylation of benzene agrees well with the absorption of the Au surface plasmon band in visible region (in figure 3).

To further check the photocatalysis of the as-prepared Au/ZnO composites, similar experiments for hydroxylation

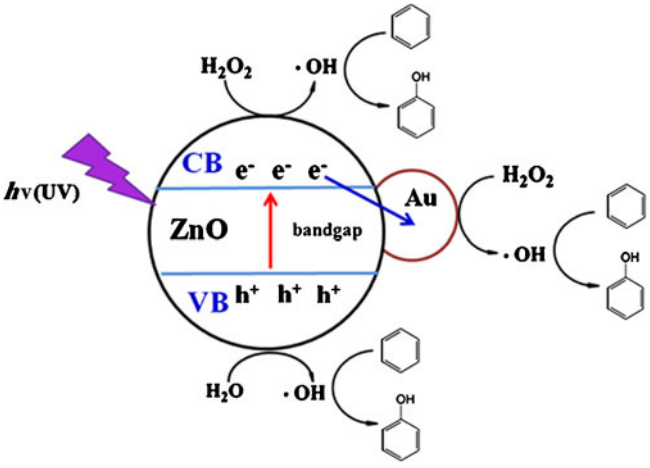


**Scheme 2.** Proposed mechanism of photocatalysis of as-prepared Au/ZnO composites under UV light irradiation.

of benzene as that under visible light irradiation were carried out using Au/ZnO composites and ZnO NPs as photocatalysts with UV light. The result of photocatalytic selectivities (◀, ▶ in figure 4a) and conversions (◀, ▶ in figure 4b) are presented in figure 4. As it can be seen, the curves (◀, ▶ in figure 4a) show that the selectivities to phenol also maintain 100% and the curves (◀, ▶ in figure 4b) obviously present that the Au/ZnO composites display higher photocatalytic activity (after 24 h, the conversion is found to be about 21·5%) than ZnO NPs (the conversion is found to be about 9·8% after 24 h) in the reaction range, which indicates that the Au/ZnO composites possess better photocatalytic performance for hydroxylation of benzene than ZnO NPs. The result demonstrates that Au NPs supported that ZnO NPs can enhance the photocatalytic ability of ZnO nanocrystals for hydroxylation of benzene while ZnO NPs are only responsible for the high selectivity to phenol. The photocatalytic response for hydroxylation of benzene agrees with absorption of the as-prepared two samples in UV region (in figure 3). From the above experimental results, a reasonable rationalization, which is similar to that in $C_{60}$/ZnO (or $TiO_2$) composites photocatalysis (Sumanta *et al* 2004; Long *et al* 2009; Xu *et al* 2010), is shown in scheme 2. In this case, first ZnO NPs were excitated by UV light with photons with energy larger than the

bandgap (3·3 eV based on the calculation from figure 3) leading to the generation of electrons in the semiconductor conduction band and electron holes in valence band. The photoinduced electron in the conduction band would transfer to Au NPs acting as electron buffer, which can hinder electron–hole pairs recombination. The long-lived electron-hole pairs are prone to generate a larger amount of photoreactive species, such as O*, with very strong oxidation ability (Xu *et al* 2010), which may account for the higher photocatalytic activity of the Au/ZnO composites than that of bare ZnO NPs.

It was found that Au/ZnO nanocomposites display higher photocatalytic activity than the individual ZnO NPs. The homogeneous component of Au NPs in the nanocomposites is considered to play an important role in the photocatalytic process. The unique property of enhancing photocatalytic activity may be ascribed to the synergetic effect and specific charge-transfer kinetics in the as-synthesized Au/ZnO nanocomposite (Li *et al* 2011).

## 4. Conclusions

In summary, the photoreactive Au/ZnO nanocomposites have been prepared by alcoholysis. For the first time, the as-synthesized Au/ZnO nanocomposites were used for photocatalytic hydroxylation of benzene. The results of photocatalytic experiments exhibit that Au NPs supported that ZnO NPs can enhance photocatalytic activity of ZnO nanocrystals in the photocatalytic process, while ZnO NPs are only responsible for the high selectivity to phenol. In addition, we found that the photocatalytic process would follow different mechanisms when different light source (UV or visible light) irradiations are used. Two different photocatalytic mechanisms are proposed depending on two important roles of Au NPs under UV or visible light irradiation. One is that Au NPs act as electrons reservoir and hinder the electron-hole pairs recombination. More importantly, the other mechanism is that Au NPs act as light harvester and catalytic active sites. Apparently our work might be helpful to improve the application of this type of heterogeneous catalysts in photocatalysis.

## Acknowledgements

This work is supported by National Basic Research Program of China (973 Program) (No. 2012CB825800), National Natural Science Foundation of China (NSFC) (Nos. 51132006, 21073127, 21071104, 20801010, 20803008, 91027041), a foundation for the author of National Excellent Doctoral Dissertation of P R China (FANEDD) (No. 200929) and a project funded by the Priority Academic Program Development of Jiangsu Higher Education Institutions (PAPD).

## References

Akyol A, Yatmaz H C and Bayramoglu M 2004 *Appl. Catal. B* **54** 19
Bell A T 2003 *Science* **299** 1688
Beqa L, Singh A K, Fan Z, Senapati D and Ray P C 2011 *Chem. Phys. Lett.* **512** 237
Bhaumik A and Kumar R 1995 *J. Chem. Soc. Chem. Commun.* 349
Bhaumik A, Mukherjee P and Kumar R 1998 *J. Catal.* **178** 101
Chakrabarti S and Dutta B K 2004 *J. Hazard. Mater.* **112** 269
Corma A and Serna P 2006 *Science* **313** 332
Donkova B, Vasileva P, Nihtianova D, Velichkova N, Stefanov P and Mehandjiev D 2011 *J. Mater. Sci.* **46** 7134
Fortuin J P and Waterman H I 1953 *Chem. Eng. Sci.* **2** 182
Hughes M D *et al* 2005 *Nature* **437** 1132
Kabra K, Chaudhary R and Sawhney R L 2004 *Ind. Eng. Chem. Res.* **43** 7683
Kang Z H, Wang E B, Mao B D, Su Z M, Gao L, Nu L, Shang H Y and Xu L 2006 *Appl. Catal. A: General* **299** 212
Kang Z H, Liu Y, Tsang C H A, Ma D D D, Wang E B and Lee S T 2009 *Chem. Commun.* **4** 413
Kurtz M, Strunk J, Hinrichsen O, Muhler M, Fink K, Meyer B and Wöll C 2005 *Angew. Chem. Int. Ed.* **44** 2790
Li P, Wei Z, Wu T, Peng Q and Li Y D 2011 *J. Am. Chem. Soc.* **133** 5660
Liu X Y, Li C H and Che C M 2006 *Org. Lett.* **8** 2707
Long Y Z, Lu Y, Huang Y, Peng Y, Lu Y, Kang S Z and Mu J 2009 *J. Phys. Chem. C* **113** 13899
Manfred W, Markus W and Michael K B 2004 *Ullmann's encyclopedia of industrial chemistry* (Germany: Wiley-VCH)
Silva C G, Juárez R, Marino T, Molinari R and García H 2011 *J. Am. Chem. Soc.* **133** 595
Strunk J, Kähler K, Xia X Y, Comotti M, Schüth F, Reineckec T and Muhler M 2009 *Appl. Catal. A: Gen.* **359** 121
Sumanta B, Subhas C B and Mana B 2004 *J. Phys. Chem. A* **108** 10783
Sun J M and Bao X H 2008 *Chem. Eur. J.* **14** 7479
Tarek A and Anja-Verena M 2009 *J. Mater. Sci.* **44** 3218
Turner M, Golovko V B, Vaughan O P H, Abdulkin P, Berenguer-Murcia A, Tikhov M S, Johnson B F G and Lambert R M 2008 *Nature* **454** 981
Wang J C, Liu P, Fu X Z, Li Z H, Han W and Wang X X 2009 *Langmuir* **25** 1218
Wang Z L 2008 *ACS Nano.* **2** 1987
Xu Y J, Zhuang Y B and Fu X Z 2010 *J. Phys. Chem. C* **114** 2669
Zhang J L, Yang C G and He C 2006 *J. Am. Chem. Soc.* **128** 1798